

## Extinction analysis of dielectric multilayer microspheres

Alla Petukhova, Andrew S. Paton, Ilya Gourevich, and Eugenia Kumacheva<sup>a)</sup>  
*Department of Chemistry, University of Toronto, 80 Saint George Street, Toronto, Ontario M5S 3H6, Canada and Institute for Optical Sciences, University of Toronto, 60 Saint George Street, Suite 331, Toronto, Ontario M5S 1A7, Canada*

Jarkko J. Saarinen and John E. Sipe  
*Department of Physics, University of Toronto, 60 Saint George Street, Toronto, Ontario M5S 1A7, Canada and Institute for Optical Sciences, University of Toronto, 60 Saint George Street, Suite 331, Toronto, Ontario M5S 1A7, Canada*

(Received 16 August 2006; accepted 11 October 2006; published online 21 November 2006)

This letter reports optical properties of spherical dielectric particles with alternating layers of high and low refractive indices. The authors “pre-designed” and synthesized polymer microspheres with alternating polystyrene and poly(trifluoroethyl methacrylate) layers of various thicknesses. Extinction of the microspheres was examined in a broad spectral range. A multipole expansion of electromagnetic field was applied for calculating the extinction efficiency of the particles. Excellent agreement was obtained between experimental and theoretical extinction curves. © 2006 American Institute of Physics. [DOI: 10.1063/1.2397031]

Multilayer dielectric particles with a periodic radial variation in refractive index can confine light through Bragg reflection. The wavelength regime of confinement can be estimated by using the Bragg condition for planar structures: the central wavelength of the confinement range is given by  $\lambda_0 = 2nd$ , where  $\lambda_0$  is the wavelength in vacuum,  $n$  is the average refractive index of the layers, and  $d$  is the period (typically two layers) of the modulation of refractive index.<sup>1-3</sup> The multilayer spheres can thus act as optical microcavities, e.g., by inhibiting or enhancing spontaneous emission of dyes or semiconductor nanocrystals (quantum dots) localized in the center of the particles.

In particles with a sufficiently large number of layers one can expect interesting optical properties even for a weak modulation in the refractive index between the layers.<sup>1,4,5</sup> This applies to polymer multilayer microspheres (PMMs) for which a typical refractive index difference between the layers is in the range from 0.1 to 0.3.<sup>4-6</sup> In order to design the PMMs, it is useful to predict the optical properties of the multilayer particles for a particular wavelength of light, using the thickness, the number, and the refractive indices of the layers.

Generally, experimental analysis of the multilayer structures relies on the measurements of scattering and extinction: the angular momentum components of the scattered field exhibit well-defined peaks. The  $Q$  factors of the different cavity quasimodes are obtained from the half-widths of these peaks.<sup>7</sup> Theoretical scattering and extinction cross sections of the multilayer structures are calculated using a multipole expansion<sup>8</sup> of the electromagnetic field by applying the boundary conditions at each interface. This is followed by the calculations of the scattering and extinction efficiencies ( $Q_{sc}$  and  $Q_{ext}$ , respectively), i.e., the scattering and extinction cross sections are divided by the geometrical cross section for a linearly polarized plane wave excitation as

$$Q_{sc} = \frac{2}{x^2} \sum_{l=1}^{\infty} (2l+1)(|a_l|^2 + |b_l|^2), \quad (1)$$

$$Q_{ext} = \frac{2}{x^2} \sum_{l=1}^{\infty} (2l+1)\text{Re}\{a_l + b_l\}, \quad (2)$$

where  $x$  is a dimensionless size parameter;  $x = k_0 a$ , where  $k_0 = 2\pi/\lambda_0$  is the wave number in vacuum, and  $a$  is the radius of the particle. The scattering coefficients  $a_l$  and  $b_l$  give the ratio between the multipole coefficients of the scattered field and those of the incident field.

All the measurable quantities related to scattering and absorption by the multilayer particles can be determined from coefficients  $a_l$  and  $b_l$ . For an isotropic sphere such an analysis reduces to the classical Mie theory.<sup>9</sup>

A straightforward calculation of the scattering coefficients  $a_l$  and  $b_l$  requires the use of the Riccati-Bessel functions; however, the numerical evaluation of these functions easily encounters instabilities.<sup>10</sup> Here we applied the recursive algorithm by Yang<sup>11</sup> to calculate the scattering coefficients.

Figure 1 shows schematically the design of the polymer microspheres used in the present work. Particles of series A and B had a multilayer structure. The experimental variables included the refractive index, the thickness, and the number of the alternating layers in the microspheres. Particles with a uniform homogeneous structure (series C) were used as a control system.

Polymer microspheres were synthesized by surfactant-free starve-fed multistage emulsion polymerization.<sup>4,5</sup> All particles were obtained in three separate polymerization stages. Polystyrene (PS) and poly(trifluoroethyl methacrylate) (PTFEMA) were used as the high and low refractive index polymers, respectively. The PMMs of series A and B were obtained by engulfing a 200 nm size PS core with a PTFEMA layer ( $n = 1.437$  at  $\lambda_0 = 589$  nm) and a PS layer ( $n = 1.592$  at  $\lambda_0 = 589$  nm).<sup>6</sup> In series A, a PS core was surrounded with a 100-nm-thick PTFEMA layer and a 400 nm PS layer. In series B, a PS core was coated with a

<sup>a)</sup>Electronic mail: ekumache@chem.utoronto.ca

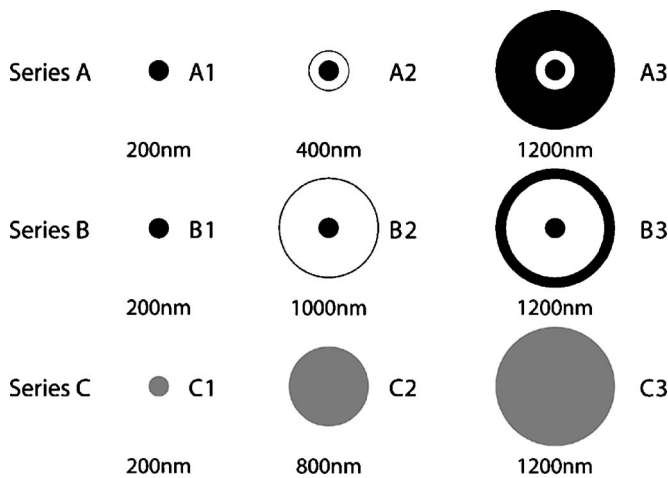


FIG. 1. Design of the polymer particles used in the present study: High refractive index polymer (black), low refractive index polymer (white), and intermediate refractive index (gray).

400-nm-thick PTFEMA layer and a 100 nm-thick PS layer. Poly(methylmethacrylate) (PMMA) particles (series C) had a homogeneous structure and a refractive index  $n=1.489$  at  $\lambda_0=589$  nm, which was approximately equal to the average refractive index of PS and PTFEMA.

Table I summarizes the targeted and experimentally measured diameters of the PMMs and the thicknesses of layers of high and low refractive indices. The particles A3, B3, and C3 had the same diameter of  $1.2 \mu\text{m}$  and the polydispersity [coefficient of variance (CV)] of the particles below 4.7%.

Figure 2 shows typical transmission electron microscopy (TEM) micrographs of the cross-sectional structure of the particles of series A3–C3 that are embedded in epoxy resin. For imaging purposes (that is, to achieve a higher contrast between the epoxy resin matrix and the microspheres), an additional PTFEMA layer was synthesized around the particles. The microbeads of series A and B have a well-defined multilayer structure and feature a sharp interface between the adjacent layers. The spherical shape of all microspheres was confirmed by using scanning electron microscopy. The surface roughness of the microspheres did not exceed 15 nm.

The extinction spectra of the particles were measured in the range from 300 to 1100 nm using a Varian Cary 5000 spectrophotometer. Prior to the measurements we ensured that the dispersions of the microspheres were sufficiently diluted to avoid multiple scattering. Figure 3 shows the measured and theoretical extinction spectra of microspheres. The

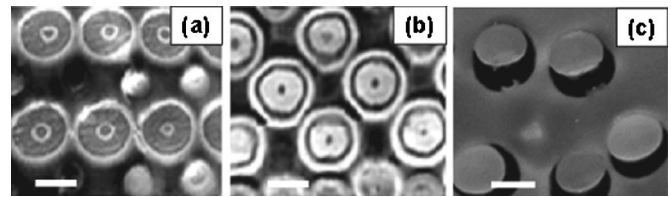


FIG. 2. TEM micrographs of microtomed polymer particles embedded in epoxy resin. PTFEMA and PS appear as the bright and dark phases, respectively. As opposed to Fig. 1, an additional PTFEMA layer is synthesized around the outside PS layer to enhance optical contrast between the particles and the epoxy resin matrix. (a) A 200 nm size PS core is engulfed with a 100-nm-thick PTFEMA layer and a 400 nm PS layer. (b) A 200 nm size PS core is engulfed with a 400-nm-thick PTFEMA layer and a 100 nm PS layer. (c) PMMA particles with a homogeneous structure. The scale bar is  $1.2 \mu\text{m}$ .

theoretical extinction efficiency was calculated by applying the recursive algorithm.<sup>11</sup> The dispersion in the refractive index in both the constituent polymers and the water medium was included in the calculation. A complex refractive index of the constituent polymers was measured using spectroscopic ellipsometry (Sopra GES-5). In Fig. 3 excellent agreement was achieved between theoretically and experimentally measured extinction spectra: the difference between the extinction efficiencies did not exceed 10%. With increasing number of layers in the PMMs (series A and B), a difference evolved between the extinction spectra of the particles. The spectrum of the microspheres with a 400-nm-thick outmost PS layer (series A3) had an extinction maximum at approximately 500 nm while the spectra of the particles with a 100-nm-thick outer PS layer (series B3) showed a band centered at 370 nm. Furthermore, the extinction spectra of particles of series A were substantially broader than the spectra of particles of series B.

A notable 130 nm redshift and the broadening of extinction spectra resulted from the difference in the PMM structure: for the same type and number of interfaces, the path of light in the low and high refractive index layers was different. The contribution of the path with a particular refractive index was further extracted by comparing the extinction spectra of particles of series B3 and C3. The average refractive index of the former was calculated as  $n_{B3}^2 = n_{PS}^2 \phi_{PS} + n_{PTFEMA}^2 \phi_{PTFEMA}$ , where  $n_{PS}$  and  $n_{PTFEMA}$  are the refractive indices, and  $\phi_{PS}$  and  $\phi_{PTFEMA}$  are the volume fractions of PS and PTFEMA, respectively. The value of  $n_{B3}$  of 1.509 (series B3) was close to 1.489, the refractive index of the uniform PMMA microspheres and the extinction peaks of particles of series B3 and C3 were separated by only a few nanometers.

TABLE I. Theoretical and experimental average diameters,  $D_t$  and  $D_{av}$ , respectively, coefficient of variation, CV, and theoretical and experimental thicknesses of layers,  $\delta_t$  and  $\delta_{ex}$ , respectively, of the polymer particles.

Sample series	$D_t$ (nm)	$D_{av}$ (nm)	CV (%)	$\delta_t$ (nm)	$\delta_{ex}$ (nm)
A1	200	209	3.5	...	...
A2	400	381	3.13	100	86
A3	1200	1143	1.19	400	381
B1	200	195	3.07	...	...
B2	1000	975	1.35	400	383
B3	1200	1211	1.82	100	118
C1	200	172	4.67	...	...
C2	800	774	3.94	300	301
C3	1200	1176	2.16	200	201

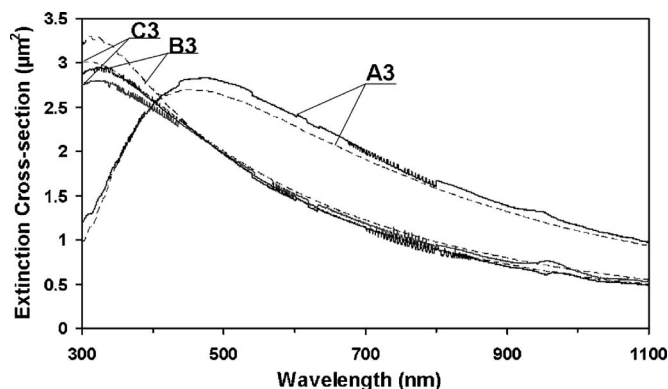


FIG. 3. Experimental and calculated (solid and dashed lines, respectively) extinction efficiency spectra for particle series A3, B3, and C3 in water. The diameters of microbeads are as in Table I. Theoretical spectra were calculated using the experimentally measured dimensions of microspheres. The experimental spectra are normalized by the path length of light ( $=1$  cm) and the concentration particles that were determined as the number of particles per unit volume ( $\approx 10^6$  cm $^{-3}$ ).

Scattering theory allows for the separation of the scattering and absorption components of the total extinction efficiency. Since absorption of both PS, PTFEMA, and PMMA occurs below 300 nm, the scattering dominated over the extinction of particles of series A3–C3. As a result, for wavelengths longer than 300 nm, the contribution of absorption to the total extinction was less than 5%. Therefore, in the region of interest, our curves accurately represent the scattering properties of the multilayer dielectric microspheres, as well as the extinction properties.

In summary, a multipole expansion of electromagnetic fields was used for calculating the extinction of spherical polymer particles with alternating layers of high and low refractive indices. Excellent agreement was obtained between the theoretical and experimental analyses of the extinction of the microspheres. The samples studied allowed us to distinguish the role of average dielectric constant (series A and B) and the role of the layered structure (series B and C). The largest difference in extinction and scattering was due to differences in the refractive index. We conclude that for a small refractive index contrast a larger number of layers would be necessary to observe an optical effect due to Bragg reflection.

This work was supported by NSERC Canada under the AGENO program.

<sup>1</sup>D. J. Brady, G. C. Papen, and J. E. Sipe, *J. Opt. Soc. Am. B* **10**, 644 (1993).

<sup>2</sup>Kevin G. Sullivan and Dennis G. Hall, *Phys. Rev. A* **50**, 2701 (1994).

<sup>3</sup>Kevin G. Sullivan and Dennis G. Hall, *Phys. Rev. A* **50**, 2708 (1994).

<sup>4</sup>A. Alteheld, I. Gourevich, L. M. Field, C. Paquet, and E. Kumacheva, *Macromolecules* **38**, 3301 (2005).

<sup>5</sup>I. Gourevich, L. M. Field, Z. Wei, C. Paquet, A. Petukhova, A. Alteheld, E. Kumacheva, J. J. Saarinen, and J. E. Sipe, *Macromolecules* **39**, 1449 (2006).

<sup>6</sup>J. Brandrup, E. H. Immergut, and E. A. Grulke, *Polymer Handbook*, 4th ed. (Wiley, New York, 1999), Vol. VI, p. 57.

<sup>7</sup>C. F. Bohren and D. R. Huffman, *Absorption and Scattering of Light by Small Particles* (Wiley, New York, 1983), pp. 83–129.

<sup>8</sup>J. D. Jackson *Classical Electrodynamics*, 3rd ed. (Wiley, New York, 1983), pp. 739–755.

<sup>9</sup>G. Mie, *Ann. Phys.* **25**, 377 (1908).

<sup>10</sup>H. Du, *Appl. Opt.* **43**, 1951 (2004).

<sup>11</sup>W. Yang, *Appl. Opt.* **42**, 1710 (2003).